LETTER

doi:10.1038/nature09713

Directed self-assembly of a colloidal kagome lattice

Qian Chen[1], Sung Chul Bae[1] & Steve Granick[1,2,3]

A challenging goal in materials chemistry and physics is spontaneously to form intended superstructures from designed building blocks. In fields such as crystal engineering[1] and the design of porous materials[2–4], this typically involves building blocks of organic molecules, sometimes operating together with metallic ions or clusters. The translation of such ideas to nanoparticles and colloidal-sized building blocks would potentially open doors to new materials and new properties[5–7], but the pathways to achieve this goal are still undetermined. Here we show how colloidal spheres can be induced to self-assemble into a complex predetermined colloidal crystal—in this case a colloidal kagome lattice[8–12]—through decoration of their surfaces with a simple pattern of hydrophobic domains. The building blocks are simple micrometre-sized spheres with interactions (electrostatic repulsion in the middle, hydrophobic attraction at the poles, which we call 'triblock Janus') that are also simple, but the self-assembly of the spheres into an open kagome structure contrasts with previously known close-packed periodic arrangements of spheres[13–15]. This open network is of interest for several theoretical reasons[8–10]. With a view to possible enhanced functionality, the resulting lattice structure possesses two families of pores, one that is hydrophobic on the rims of the pores and another that is hydrophilic. This strategy of 'convergent' self-assembly from easily fabricated[16] colloidal building blocks encodes the target supracolloidal architecture, not in localized attractive spots but instead in large redundantly attractive regions, and can be extended to form other supracolloidal networks.

Colloidal crystals are important for their proposed applications in photonics, biomaterials, catalytic supports and lightweight structural materials. They also serve as model systems in which to study the phase behaviour and crystallization kinetics of atomic and molecular crystals[13–15]. Usually composed of hard spheres that are homogeneous in surface functionality, their spontaneous formation is mostly induced by the minimization of entropy, which results in a limited selection of attainable close-packed crystal types[13–15]. More complex crystals assembled from similarly homogeneous spheres have been constructed in binary colloidal[17] and template-assisted systems[18]. To achieve programmable formation of crystals, building blocks with designed specific surface functionalities such as DNA linkers[19,20] and attractive 'patches'[5–7,21,22] have been proposed, but these approaches pose synthetic challenges and can be difficult to generalize. For example, the kagome lattice (see Fig. 1), which is of theoretical interest for mathematical reasons[8] as well as its relevance to mechanical stability of an isostatic lattice[9] and frustration in magnetic materials[10], is composed of interlaced triangles whose vertices have four contacting neighbours. To construct it by direct assembly would require colloids with four unevenly distributed patches on their equators to line up precisely with their counterparts on neighbouring spheres (see Supplementary Fig. 1a) but methods to obtain the desired colloids are not immediately accessible.

Accordingly, we chose the kagome lattice as our target colloidal crystal, and produce it using the following alternative strategy. To reduce the need to start with a specific pattern of attractive spots on each building block, we designed a building block with the orthogonal attributes of minimal surface design combined with self-adjusted coordination number. This simplifies the original four-patch decoration scheme into one with two patches at opposite poles, each of which subtends an angle in the plane large enough to allow coordination with two nearest neighbours (see Supplementary Fig. 1b). This has the advantage that established synthetic methods[16] can be used to decorate spherical particles with two hydrophobic poles of tunable area, separated by an electrically charged middle band. Because each of the hemispheres is chemically 'Janus' (two-sided)[23] with the same middle band, we refer to these as 'triblock Janus'.

This motif causes neighbouring particles to attract at their poles in a geometrical arrangement limited by their size, while avoiding energetically unfavourable contacts between the charged middle bands. After overnight sedimentation, the density mismatch between our gold-plated polystyrene particles and the water in which they are suspended concentrates the particles into a quasi-two-dimensional system. Our synthetic scheme produces elongated caps (see Supplementary Fig. 2), which further facilitates assembly into two-dimensional networks because it allows two nearest neighbours only when the long patch axes of neighbouring particles are parallel. Ordering is then switched on at will by adding salt (3.5 mM NaCl in these experiments) to these spheres in

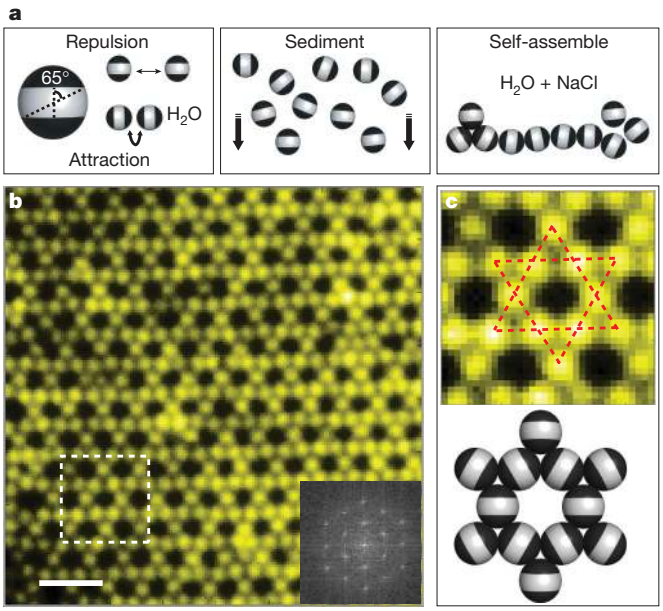

Figure 1 | Colloidal kagome lattice after equilibration. **a**, Triblock Janus spheres hydrophobic on the poles (black, with an opening angle of 65°) and charged in the equator section (white), are allowed to sediment in deionized water. Then NaCl is added to screen electrostatic repulsion, allowing self-assembly by short-range hydrophobic attraction. **b**, Fluorescence image of a colloidal kagome lattice (main image) and its fast Fourier transform image (bottom right). Scale bar is 4 μm. The top panel in **c** shows an enlarged view of the dashed white rectangle in **b**. Dotted red lines in **c** highlight two staggered triangles. The bottom panel in **c** shows a schematic illustration of particle orientations.

[1]Department of Materials Science and Engineering, University of Illinois, Urbana, Illinois 61801, USA. [2]Department of Chemistry, University of Illinois, Urbana, Illinois 61801, USA. [3]Department of Physics, University of Illinois, Urbana, Illinois 61801, USA.

deionized water; the salt screens electrostatic repulsions and allows hydrophobic attraction to come into play. The successful completion of the ordering process requires the energy landscape of the system to be smooth enough for kinetically favoured intermediates to transform finally to the thermodynamically favoured product with maximized hydrophobic contacts. Experimentally, the hydrophobic attraction of around $10k_BT$ (where k_B is the Boltzmann constant and T is temperature) per contact[23] allows self-correction of imperfectly aligned bonds, which is advantageous because kinetically formed intermediate defects finally transform to the favoured structure over a convenient timescale. The scheme of self-assembly is summarized in Fig. 1a.

Fluorescence images of the final product (Fig. 1b) reveal single-phase web-like sheets that tessellate the surface in the known pattern of a kagome lattice. Interestingly, the two populations of pores in this lattice, triangular and hexagonal, each possess inherently different microenvironments on the pore rims. As demonstrated in Fig. 1c, hexagonal cavities are surrounded by negatively charged rims and triangular cavities are surrounded by hydrophobic rims. Previously, others have succeeded in forming kagome lattices when functional molecules self-assemble epitaxially onto certain metals[11], but our substrate is essentially inert; it simply carries negative charge in order to prevent colloids from sticking to it. Accordingly, a key difference from such molecular systems is that lateral positions of elements of the kagome lattice display thermal fluctuation around their mean positions, as shown in Supplementary Movie 1. In principle, this should enable direct measurement of the vibration modes and phonon structure[24], which are of interest theoretically[9]. Although it might seem obvious which structure we will observe, computer simulations of similar particles show a different structure, close-packed with alternating attractive bands[21]. The key difference appears to be that experimentally, particles were free to exchange outside the monolayer. This contrast between experiment and simulation implies that different crystal structures should be observed at low and high pressure. We anticipate another phase transition—melting—if the attraction were weaker, as could be achieved experimentally by using a mixed monolayer of alkane thiols instead of the strongly hydrophobic monolayers used here.

We now follow the ordering process, which is difficult to do with surface-templated systems. Defining the start of the experiment as the moment when salt is added, fluorescence imaging shows that particles first recognize the existence of neighbours by clustering into kinetically favoured triangles, strings or a combination of the two. Subsequently, they rapidly coordinate with additional particles to maximize contacts between hydrophobic poles, resulting in chunks of network with defects consisting mainly of irregular voids. A typical early-stage image is shown in Fig. 2a. The sample at this time contains some web-like structures (Fig. 2b) and other strings with dangling bonds (Fig. 2c). Quantitative analysis of their relative abundance (Fig. 2d) shows, with elapsed time, a monotonic decrease of monomers, a monotonic increase of web-like structures, and a peak in the abundance of strings; hence, strings are a kinetically favoured intermediate that does not require patch alignment as accurate as in webs and that has more translational and rotational freedom. In Supplementary Movie 2, we follow the typical evolution of a string first into triangular nodes with branches, then into enclosed pores. The particle number density in this movie is smaller than in Fig. 2a to demonstrate individual dynamic events. This system behaves similarly to the pattern in Fig. 2d at this stage of assembly, but at a slower rate.

For the kagome lattice to develop fully requires much longer. After the formation of irregular webs, the colloids first adopt quasi-kagome order in local areas, which then extend. This growth of the final structure from metastable intermediates suggests that classical nucleation theory for the (well-studied) crystallization of closely packed spheres should be revisited; in this system, in determining the size and shape of critical nuclei, the concept of average surface tension may be quantitatively or even qualitatively different. To quantify the ordering process,

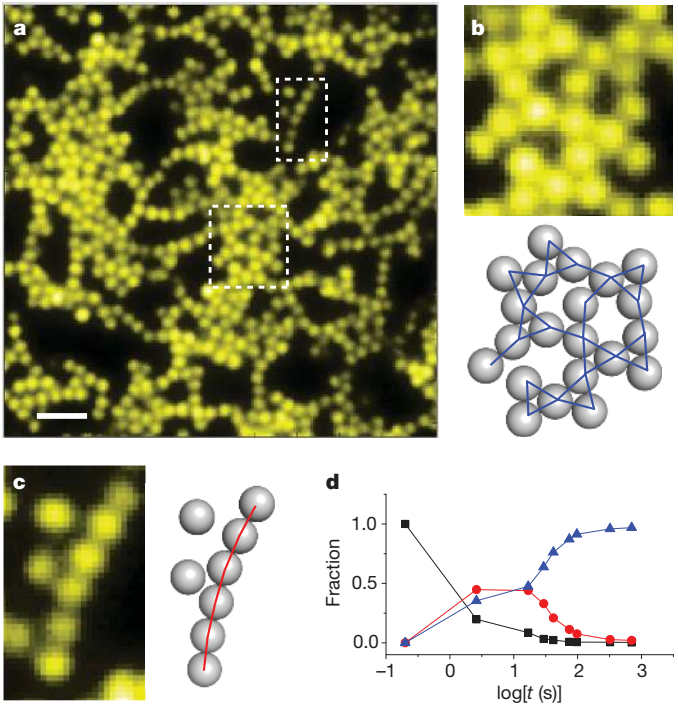

Figure 2 | Stages of self-assembly of kagome lattice. **a**, Illustrative fluorescence image taken 35 s after initiation of assembly. Scale bar is 4 μm. **b**, **c**, Enlarged views of a web-like area (**b**) and a single-particle string area (**c**), both highlighted in **a** by dashed white rectangles. Bonding types are shown in the accompanying schematic illustrations (blue lines in **b** and red lines in **c**). **d**, Time evolution of structures illustrated in **a**–**c**, showing the relative abundance of discrete spheres (black squares), strings (red circles), and triangular bonding (blue triangles). The time spans 0.2 s to 12 min.

for each particle in each time sequence of images, we determined and then quantified the local coordination of each particle to its neighbours using the local bond orientational order parameter ψ_{6j}. Particles with four bonds and ψ_{6j} larger than 0.7 were defined as locally crystalline[14].

Figure 3 consists of a time series of images, showing isolated crystal bonding, then fusion into larger domains, and finally healing of non-crystalline bonds into ordered ones. The crystalline domains fluctuate, making the edges across ordered and random regions rough and sometimes transient (Supplementary Movie 3). The graph in Fig. 3e characterizes the average of images of this kind and shows the time dependence. Interestingly, the approach follows typical first-order chemical reaction kinetics, during which time the particle number density remains nearly constant, with the fraction of product increasing rapidly at first, then more slowly as the available materials are depleted, and finally saturating exponentially to a plateau. Together with the earlier stage in which individual particles condense into irregular networks (Fig. 2 and Supplementary Movie 2), this is reminiscent of two-step nucleation in protein solutions, in which order is preceded by a dense amorphous state[25]. Eventually, we find that growing crystalline grains of different orientations impinge on one another. Supplementary Fig. 3 shows examples of long-range crystalline order, at dilute and concentrated concentrations. This polycrystalline structure could be annealed and its order improved by the usual methods of materials science.

Furthermore, sheets of kagome lattice are found to stack, one above the other, in parallel layers. In a bilayer, both layers retain the in-plane order of a kagome lattice: in registry but staggered in orientation, so that the intersection of nodes of the two lattices forms an octahedron. An optical image of the resulting array of octahedra is shown in Fig. 4. This stacking maximizes the hydrophobic node comprised of six hydrophobic poles in each octahedron; alternative arrangements would be more costly in energy, requiring hydrophobic nodes in one plane to be positioned over the pores with charged rims in the second

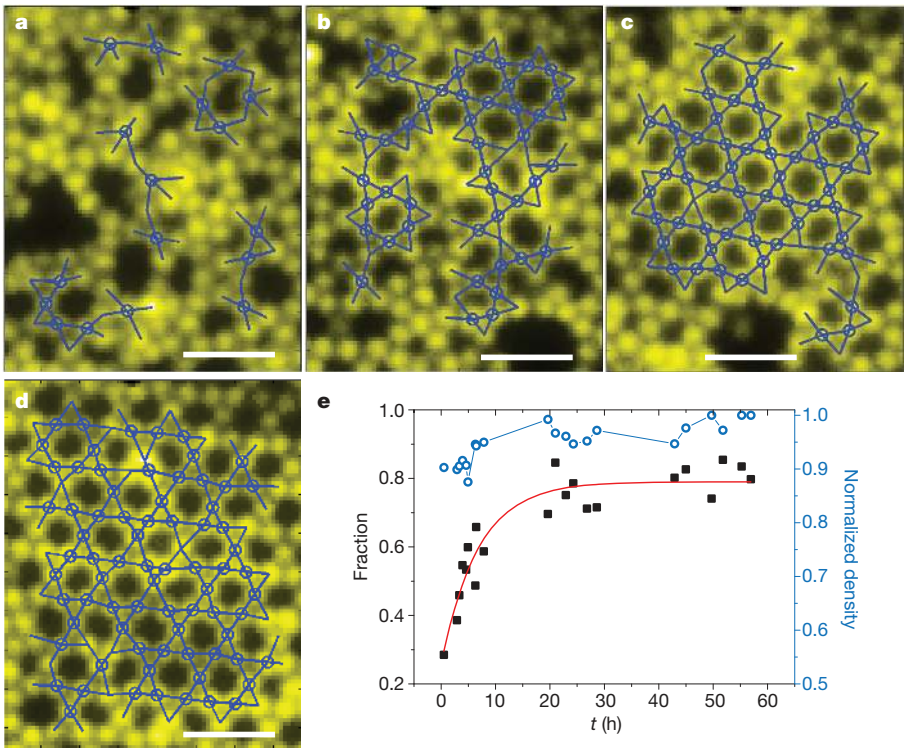

Figure 3 | Crystallization of the kagome lattice. Fluorescence images taken at 2.9 h, 3.0 h, 3.1 h and 53.8 h (**a**, **b**, **c** and **d**, respectively). Blue circles denote the particles of local crystalline order as defined in the text. Blue lines are their neighbouring bonds. Scale bar is 4 μm. **e**, The time evolution of the fraction of particles bearing local crystalline order (black squares), corrected for particles with missing bonds at the boundary, which approaches a plateau with exponential kinetics (red line). Also shown is the particle number density (blue circles), normalized by its observed maximum.

plane. Although technical limitations in visualizing the resulting structure at present prevent us from visualizing the assembly to still thicker films, there is the potential to fabricate multilayers of vertex-sharing octahedral, pyrochlore and other hierarchical structures usually associated with inorganic crystals rather than colloids[8]. Looking ahead to possible applications, freezing these structures into place offers the potential to form selective membranes, in which some holes are hydrophobic and others hydrophilic.

These design rules suggest generalizations. Other open structures[26] could be designed from triblock particles the coordination numbers of which differ on the opposing north and south poles. The needed modulation of the angular range of attraction could be achieved by lessening the size of the hydrophobic patch, or alternatively by less screening of repulsion. If building blocks were to carry four attractive patches distributed at tetrahedral angles, a diamond structure would be artificially designed, although implementation of this awaits the development of the synthetic methods needed to produce the parent particles[27]. The common point is that colloidal building blocks, attracting one another reversibly, during the early stages of assembly assemble into intermediate clusters (strings, in the present experiments) with wide latitude in the mutual orientation of neighbouring particles. Subsequently, the orthogonal variable of geometrical shape then guides these transiently stable intermediates to the final structure.

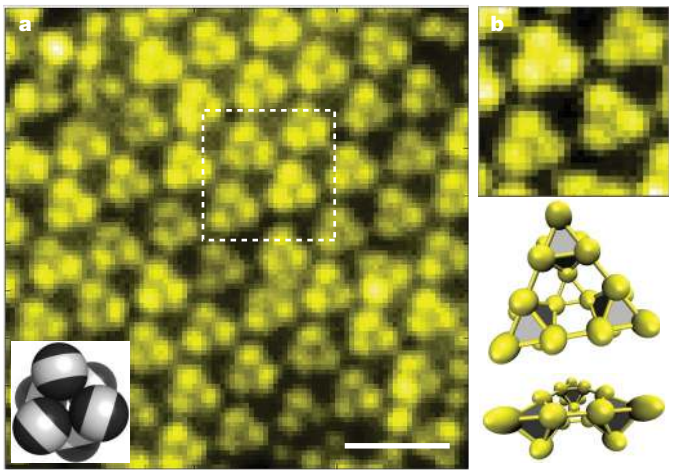

Figure 4 | A bilayer of parallel kagome lattices. **a**, Fluorescence image taken from the bottom. The eye sees octahedra consisting of staggered triangular nodes, as shown in the schematic illustration at bottom left. Scale bar is 4 μm. **b**, Enlarged view of the dashed white square in **a**. The top panel in **b** shows a fluorescence image. The bottom panel in **b** shows a schematic view of particle arrangements from two perspectives, nearly vertical to the plane and nearly parallel to it.

METHODS SUMMARY

Fluorescent latex particles of sulphate polystyrene (1 μm in diameter, F-8851 from Invitrogen) are made hydrophobic on opposite poles through glancing angle deposition of titanium (2 nm) and gold (25 nm) thin films, followed by the deposition of self-assembled monolayers of *n*-octadecanethiol (Sigma-Aldrich). After adding salt (NaCl) to deionized water to a final concentration of 3.5 mM, their self-assembly is observed at room temperature under epifluoresence microscopy. Images captured by an iXon electron multiplying charge coupled device (EMCCD) camera are analysed manually for the early stage of self-assembly, and by single-particle tracking code after particles begin to form web-like structures. Because incomplete webs are only locally periodic, we use the local bond orientational order parameter, rather than a translational order parameter, to quantify the growth of ordered regions within the sample.

Full Methods and any associated references are available in the online version of the paper at www.nature.com/nature.

Received 22 July; accepted 25 November 2010.

1. Desiraju, G. R. Crystal engineering: a holistic view. *Angew. Chem. Int. Edn Engl.* **46,** 8342–8356 (2007).
2. Bartels, L. Tailoring molecular layers at metal surfaces. *Nature Chem.* **2,** 87–95 (2010).

3. Yaghi, O. M. *et al.* Reticular synthesis and the design of new materials. *Nature* **423,** 705–714 (2003).
4. Sun, Q.-F. *et al.* Self-assembled $M_{24}L_{48}$ polyhedra and their sharp structural switch upon subtle ligand variation. *Science* **328,** 1144–1147 (2010).
5. Glotzer, S. C. & Solomon, M. J. Anisotropy of building blocks and their assembly into complex structures. *Nature Mater.* **6,** 557–562 (2007).
6. Mann, S. Self-assembly and transformation of hybrid nano-objects and nanostructures under equilibrium and non-equilibrium conditions. *Nature Mater.* **8,** 781–792 (2009).
7. Liu, K. *et al.* Step-growth polymerization of inorganic nanoparticles. *Science* **329,** 197–200 (2010).
8. van der Marck, S. C. Site percolation and random walks on *d*-dimensional Kagomé lattices. *J. Phys. Math. Gen.* **31,** 3449–3460 (1998).
9. Souslov, A., Liu, A. J. & Lubensky, T. C. Elasticity and response in nearly isostatic periodic lattices. *Phys. Rev. Lett.* **103,** 205503 (2009).
10. Atwood, J. L. Kagomé lattice: a molecular toolkit for magnetism. *Nature Mater.* **1,** 91–92 (2002).
11. Schlickum, U. *et al.* Chiral Kagomé lattice from simple ditopic molecular bricks. *J. Am. Chem. Soc.* **130,** 11778–11782 (2008).
12. Glettner, B. *et al.* Liquid-crystalline Kagome. *Angew. Chem. Int. Edn Engl.* **47,** 9063–9066 (2008).
13. Yethiraj, A. & van Blaaderen, A. A colloidal model system with an interaction tunable from hard sphere to soft and dipolar. *Nature* **421,** 513–517 (2003).
14. Gasser, U., Weeks, E. R., Schofield, A., Pusey, P. N. & Weitz, D. A. Real-space imaging of nucleation and growth in colloidal crystallization. *Science* **292,** 258–262 (2001).
15. Anderson, V. J. & Lekkerkerker, H. N. W. Insights into phase transition kinetics from colloid science. *Nature* **416,** 811–815 (2002).
16. Pawar, A. B. & Kretzschmar, I. Patchy particles by glancing angle deposition. *Langmuir* **24,** 355–358 (2008).
17. Shevchenko, E. V., Talapin, D. V., Kotov, N. A., O'Brien, S. & Murray, C. B. Structural diversity in binary nanoparticle superlattices. *Nature* **439,** 55–59 (2006).
18. Xia, Y., Yin, Y., Lu, Y. & McLellan, J. Template-assisted self-assembly of spherical colloids into complex and controllable structures. *Adv. Funct. Mater.* **13,** 907–918 (2003).
19. Park, S. Y. *et al.* DNA-programmable nanoparticle crystallization. *Nature* **451,** 553–556 (2008).
20. Nykypanchuk, D., Maye, M. M., van der Lelie, D. & Gang, O. DNA-guided crystallization of colloidal nanoparticles. *Nature* **451,** 549–552 (2008).
21. Giacometti, A., Lado, F., Largo, J., Pastore, G. & Sciortino, F. Effects of patch size and number within a simple model of patchy colloids. *J. Chem. Phys.* **132,** 174110 (2010).
22. Doppelbauer, G., Bianchi, E. & Kahl, G. Self-assembly scenarios of patchy colloidal particles in two dimensions. *J. Phys. Condens. Matter* **22,** 104105 (2010).
23. Hong, L., Cacciuto, A., Luijten, E. & Granick, S. Clusters of amphiphilic colloidal spheres. *Langmuir* **24,** 621–625 (2008).
24. Ghosh, A., Chikkadi, V. K., Schall, P., Kurchan, J. & Bonn, D. Density of states of colloidal glasses. *Phys. Rev. Lett.* **104,** 248305 (2010).
25. Liu, H., Kumar, S. K. & Douglas, J. F. Self-assembly-induced protein crystallization. *Phys. Rev. Lett.* **103,** 018101 (2009).
26. Grünbaum, B. & Shephard, G. C. *Tilings and Patterns* (W. H. Freeman, 1987).
27. Kraft, D. J., Groenewold, J. & Kegel, W. K. Colloidal molecules with well-controlled bond angles. *Soft Matter* **5,** 3823–3826 (2009).
28. Li, C., Hong, G. & Qi, L. Nanosphere lithography at the gas/liquid interface: a general approach toward free-standing high-quality nanonets. *Chem. Mater.* **22,** 476–481 (2010).

Supplementary Information is linked to the online version of the paper at www.nature.com/nature.

Acknowledgements This work was supported by the US Department of Energy, Division of Materials Science, under award number DE-FG02-07ER46471 through the Frederick Seitz Materials Research Laboratory at the University of Illinois at Urbana-Champaign. For equipment, we acknowledge the National Science Foundation, CBET-0853737. We thank K. Chen for help with particle tracking.

Author Contributions Q.C. and S.G. initiated this work; Q.C. and S.G. designed the research programme; Q.C. performed the experiments; Q.C., S.C.B. and S.G. wrote the paper.

Author Information Reprints and permissions information is available at www.nature.com/reprints. The authors declare no competing financial interests. Readers are welcome to comment on the online version of this article at www.nature.com/nature. Correspondence and requests for materials should be addressed to S.G. (sgranick@illinois.edu).

METHODS

Particle fabrication. Patches on opposite poles of spherical particles are produced by sequential glancing angle deposition[16]. First, a closely packed monolayer of 1 μm fluorescent sulphated latex particles (F-8851, Invitrogen) is fabricated on a silicon wafer substrate using a reported method[28]. In brief, 80 μl water/ethanol dispersion (volume ratio 1:1) containing 8 wt% latex particles is dropped onto the top surface of a 1 cm × 1 cm piece of glass (pretreated by Piranha solution) surrounded by water located at the midbottom of a Petri dish. The dispersion spreads freely on the water surface until it covers nearly the entire area. Then 10 μl of sodium dodecyl sulphate (2 wt%) solution is added to the water surface to reduce the surface tension and condense the particles into a closely packed monolayer of about 16 cm^2 in area. A silicon wafer (1.5 cm × 2.5 cm, pretreated by Piranha solution) is used to pick a piece of floating monolayer of particles, left to dry for later treatment.

Second, glancing angle deposition of 2 nm Ti/25 nm Au layers onto the colloidal monolayer is performed as described[16]. The glancing angle θ is set to be 30° to the particle monolayer. After the first vapour deposition, the particle monolayer is lifted up with a polydimethylsiloxane (PDMS) stamp so that patches from the first vapour deposition are facing down. PDMS stamps are prepared by curing the monomer and crosslinking agent (10:1 w/w) (Dow Corning) at 70 °C in a pumped oven overnight. Just before stamping, the PDMS surface is treated with oxygen plasma to induce the necessary adhesion. The oxygen plasma is generated by a Harrick PDC-32G plasma cleaner. Low plasma power is used (6.8 W), and the chamber pressure is about 150 mTorr. The treatment duration is 45 s. The stamping is carried out immediately after the plasma treatment. Then the second deposition is performed, from the other direction of the colloidal monolayer, to produce patches on the other poles of the colloids. The PDMS stamp with colloidal particles attached is immersed in 2 mM octadecanethiol (Sigma-Aldrich) in ethanol for 7 h to render the Au coatings hydrophobic. Particles on PDMS stamp are rinsed with ethanol multiple times and then redispersed in deionized water via ultrasonication.

Self-assembly. A suspension of triblock Janus particles in deionized water is contained in a flat silica cuvette (Lab-Tek II chambered coverglass). Particles are repelled from the cuvette bottom by its negative charge. We note that the gravitational height of the as-prepared particles, $h = k_BT/mg \approx 4$ μm, concentrates the dispersed particles into a quasi-two-dimensional system after overnight sedimentation. Here, T is the room temperature and mg is the buoyant weight of the particle, considering both the density of latex particles (1.055 g cm^{-3}) and the gold coating. The range of hydrophobic attraction is short compared to our particle diameter, which the experimental literature reports to be in the range 10–100 nm and was successfully modelled with a potential decaying roughly exponentially with a decay constant of the order of 10 nm (ref. 23). This short range can enforce contact interactions, disfavouring the more loosely bound structures that will result for long-range attractions. The salt NaCl is added in order to screen repulsion to a Debye length of ~5 nm to allow the recognition of attraction between patches and their consequent self-assembly. Using epifluorescence microscopy (63× air objective with a 1.6× post magnification, numerical aperture 0.75) with an iXon EMCCD camera, we monitor the dynamic evolution of the system. We quantified this dynamical change in structure by manual mapping in Fig. 2d, and a combination of particle tracking and calculation of the local two-dimensional bond-orientational order parameter in Fig. 3e:

$$\psi_{6j} = \frac{1}{nn}\sum_{k=1}^{nn} e^{6i\theta_{jk}}$$

where nn is the number of nearest neighbours of particle j identified from Delaunay triangulation. Here θ_{jk} is the angle of the bond between particle j and its neighbour k to an arbitrary reference axis. This definition of order parameter is valid for the kagome lattice because it shares the same arrangement of neighbour orientation as a triangular lattice except for the missing particles. Meanwhile, to avoid the inclusion of particles locally ordered with six bonds as in a triangular lattice, only particles with both $\psi_{6j} > 0.7$ and four nearest-neighbouring bonds are denoted as particles with local kagome lattice order.